



Published in final edited form as:

Nature. 2012 November 15; 491(7424): 473–477. doi:10.1038/nature11626.

## Endothelial cell expression of hemoglobin $\alpha$ regulates nitric oxide signaling

Adam C. Straub<sup>1</sup>, Alexander W. Lohman<sup>1,2</sup>, Marie Billaud<sup>1,2</sup>, Scott R. Johnstone<sup>1</sup>, Scott T. Dwyer<sup>3</sup>, Monica Y. Lee<sup>1</sup>, Pamela Schoppee Bortz<sup>1</sup>, Angela K. Best<sup>1</sup>, Linda Columbus<sup>4</sup>, Benjamin Gaston<sup>3</sup>, and Brant E. Isakson<sup>1,2</sup>

<sup>1</sup>Robert M. Berne Cardiovascular Research Center, University of Virginia, Charlottesville, Virginia 22908, USA

<sup>2</sup>Department of Molecular Physiology and Biological Physics, University of Virginia, Charlottesville, Virginia 22908, USA

<sup>3</sup>Department of Pediatrics, University of Virginia, Charlottesville, Virginia 22908, USA

<sup>4</sup>Department of Chemistry, University of Virginia, Charlottesville, Virginia 22908, USA

Models of unregulated nitric oxide (NO) diffusion do not consistently account for the biochemistry of NO synthase (NOS)-dependent signaling in many cell systems<sup>1,2,3</sup>. For example, endothelial NOS (eNOS) controls blood pressure, blood flow and oxygen delivery through its effect on vascular smooth muscle tone<sup>4</sup>, but the regulation of these processes is not adequately explained by simple NO diffusion from endothelium to smooth muscle<sup>3,5</sup>. Here, we report a new paradigm in the regulation of NO signaling by demonstrating that hemoglobin (Hb)  $\alpha$  is expressed in arterial endothelial cells (ECs) and enriched at the myoendothelial junction (MEJ), where it regulates the effects of NO on vascular reactivity. Surprisingly, this function is unique to Hb  $\alpha$  and abrogated by its genetic depletion. Mechanistically, endothelial Hb  $\alpha$  heme iron in the Fe<sup>3+</sup> state permits NO signaling, and this signaling is shut off when Hb  $\alpha$  is reduced to the Fe<sup>2+</sup> state by endothelial cytochrome B5 reductase 3 (CytB5R3)<sup>6</sup>. Genetic and pharmacological inhibition of CytB5R3 increases NO bioactivity in small arteries. These data reveal a novel mechanism by which the regulation of intracellular Hb  $\alpha$  oxidation state controls NOS signaling in non-erythroid cells. This

Users may view, print, copy, download and text and data- mine the content in such documents, for the purposes of academic research, subject always to the full Conditions of use: [http://www.nature.com/authors/editorial\\_policies/license.html#terms](http://www.nature.com/authors/editorial_policies/license.html#terms)

Correspondence and requests for materials should be addressed to: Brant E. Isakson, Robert M. Berne Cardiovascular Research Center, University of Virginia School of Medicine, P.O. Box 801394, Charlottesville, VA 22908, Phone: 434-924-2093, Fax: 434-924-2828, [brant@virginia.edu](mailto:brant@virginia.edu).

### Competing financial interest

None

### Author contributions

A.C.S. performed the majority of the experiments and data analysis. A.W.L performed vessel transfections. Vascular reactivity was executed by A.W.L and M.B. S.R.J carried out immunofluorescence studies and S.T.D. assisted in NO diffusion and consumption assays. M.Y.L and P.S.B performed realtime-PCR experiments and A.K.B. helped with all cell culture experiments. L.C. performed the modeling experiments. B.G. helped with experimental design, provided use of the nitric oxide analyzer and NO, and assisted with final manuscript preparation. B.E.I. initiated, directed and supported the work through all levels of development. All the authors discussed the results and commented on the manuscript.

paradigm may be relevant to heme-containing globins in a broad range of NOS-containing somatic cells<sup>7,8,9,10,11,12,13</sup>.

Endothelial NOS modulates blood vessel diameter in response to both vasodilators and vasoconstrictors. For example, it is known that during arterial constriction NO from endothelium feeds back on smooth muscle to control the magnitude of the response to a vasoconstrictor (e.g. phenylephrine (PE))<sup>5,14</sup>. PE stimulation of thoracodorsal (TD) arteries *ex vivo* - and of primary human ECs and vascular smooth muscle cells (SMCs) in the vascular cell co-culture (VCCC) model - reproduced classical NOS- and cGMP-dependent changes in SMC biology (Supplementary Fig. 1a–d). However, NO did not diffuse into the extracellular space (Supplementary Fig. 1e–h), consistent with our previous work showing compartmentalized NOS signaling at the MEJ, the critical EC-SMC contact point in the TD and other small arteries and arterioles<sup>5</sup>. Therefore, we studied MEJ proteins that could contribute to local regulation of NO diffusion and biochemistry. We performed a proteomic analysis of MEJs isolated from VCCCs using the isobaric tags for relative and absolute quantitation (iTRAQ) system (Supplementary Fig. 2). Surprisingly, Hb  $\alpha$  was abundant at the MEJ (Supplementary Fig. 3). Because Hb can regulate NO diffusion and biochemistry in erythrocytes<sup>15,16</sup>, we hypothesized that it could have a similar function at the MEJ.

First, we confirmed the proteomic data using immunoblot and immunofluorescence. We demonstrated Hb  $\alpha$  protein expression in the VCCC model but no expression of Hb  $\beta$  (Fig. 1a). There was little Hb  $\alpha$  expression in human ECs or SMCs grown separately, and there was no Hb  $\alpha$  in the fibronectin or gelatin used to coat the VCCC transwells (Fig. 1a). Next, we confirmed these results in co-cultures of different types of ECs and SMCs where MEJs also expressed abundant Hb  $\alpha$  (Supplementary Fig. 4). We then studied the MEJ distribution of Hb  $\alpha$  *in situ*. Gold particles labeling Hb  $\alpha$  were abundant in the MEJ of mouse TD arteries visualized by transmission electron microscopy (TEM) (Fig. 1b). In contrast, carotid arteries – conduit arteries which have few MEJs - expressed little Hb  $\alpha$  as observed by TEM (Fig. 1b), immunoblot (Fig. 1c), and immunofluorescence (Fig. 1d). These data were consistent in human skeletal muscle arterioles (Fig. 1d) and throughout multiple tissue beds (Supplementary Fig. 5). Using *en face* immunofluorescence, we found punctuate Hb  $\alpha$  staining primarily at paracellular junctions of TD – but not carotid – arteries, whereas little Hb  $\beta$  was observed (Fig. 1e). Chemical crosslinking analysis revealed that the Hb  $\alpha$  was monomeric in TD arteries and the VCCC (Fig. 1f). Next, we measured Hb  $\alpha$  mRNA using real-time PCR (Fig. 1g) and established that ECs transfected with Hb  $\alpha$  siRNA had decreased protein expression at the MEJ (Supplementary Fig. 6a) and in the monolayer (Supplementary Fig. 6b). Loss of Hb  $\alpha$  protein expression did not affect eNOS expression in the EC monolayer (Supplementary Fig. 6b) or at the MEJ (Supplementary Fig. 7). Transcripts for other globins including myoglobin, neuroglobin and cytoglobin were absent in ECs (Supplementary Fig. 8a–c). Only cytoglobin mRNA and protein were expressed in SMCs (Supplementary Fig. 8c–d), consistent with a previous report<sup>11</sup>. In addition, we also found Hb  $\alpha$  stabilizing protein in the endothelium of TD arteries and in the VCCC (Supplementary Fig. 9a–b). Taken together, these data show for the first time that arterial ECs express Hb  $\alpha$  mRNA and protein and are responsible for enriched Hb  $\alpha$  expression at the MEJ.

To investigate the functional role of Hb  $\alpha$  in ECs and its effect on eNOS signaling, we transfected ECs in isolated TD arteries with Hb  $\alpha$  or control siRNA. Knockdown efficiency was 70–80% (Supplementary Fig. 10). Loss of Hb  $\alpha$  resulted in a dramatic loss in arterial reactivity following PE application in a single or cumulative doses (Fig. 2a–b) and increased reactivity to acetylcholine (Ach) (Fig. 2c), but there was no change in response to 5-hydroxytryptamine (5-HT) (Supplementary Table 1).  $EC_{50}$  and  $E_{max}$  values are in Supplementary Table 2. We observed no difference in basal tone (Supplementary Fig. 11a). However, with the addition of the NOS inhibitor L- $N^G$ -nitroarginine methyl ester (L-NAME), the effect of Hb  $\alpha$  siRNA was comparable to control conditions for both PE and Ach responses (Fig. 2a–c). We thus hypothesized that eNOS, the primary isoform in the vessel wall, may be in close spatial proximity to Hb  $\alpha$ . We tested this hypothesis using four methods: co-localization studies by immunofluorescence (Fig. 2d, g), a proximity ligation assay (Fig. 2e), and co-immunoprecipitations from cell lysates (Fig. 2f, h) and purified proteins (Fig. 2i). These analyses revealed Hb  $\alpha$  and eNOS are in a macromolecular complex and can form a direct protein-protein interaction.

Hb  $\alpha$  likely interacts with eNOS to regulate blood vessel tone by controlling NO diffusion through its scavenging by heme iron<sup>13,17,18,19</sup>. We studied the mechanism of interaction by measuring loss of NO radical in TD and carotid arteries, and in the VCCC model. NO was lost in TD arteries, but not carotid arteries; and it was lost in MEJ fractions - but not EC or SMC -lysates (Supplementary Fig. 12a–b). Next, we knocked down endothelial Hb  $\alpha$  in isolated arteries (Fig 2j) or VCCCs (Fig 2l) using siRNA. Loss of Hb  $\alpha$  increased NO diffusion across the vessel wall (Fig. 2k) and in the VCCC (Fig. 2m). Together, these results indicate that endothelial Hb  $\alpha$  can regulate arterial tone through its effects on NO diffusion.

Next, we hypothesized that Hb  $\alpha$  heme iron in the oxygenated  $Fe^{2+}$  state should control NO diffusion through a fast reaction ( $2.4 \times 10^7 \text{ M}^{-1} \cdot \text{sec}^{-1}$ )<sup>20</sup> resulting in dioxygenation<sup>21,22</sup>, whereas  $Fe^{3+}$  state should permit NO diffusion due to a slower reaction rate ( $3.3 \times 10^3 \text{ M}^{-1} \cdot \text{sec}^{-1}$ )<sup>23</sup>. We found that Hb  $\alpha$  heme iron resides in both states. First, using UV-visible spectroscopy, we identified a Soret peak (~420 nm) and Q bands (~540–575 nm) in isolated TD arteries consistent with oxygen bound Hb  $Fe^{2+}$ , whereas there was no peak in carotid arteries (Fig 3a). Next, we measured the oxidation state of Fe and found approximately 42% existed in the  $Fe^{2+}$  and 58% in the  $Fe^{3+}$  state (Fig. 3b). These measurements were sensitive to Hb  $\alpha$  siRNA (Fig. 3b). Consistent with this observation, we found that carbon monoxide (CO) ligated  $Fe^{2+}$  heme, resulted in increased NO diffusion across isolated vessels (Supplementary Fig. 12c). When MEJ fractions were studied, we found a Soret peak (~410 nm) characteristic of the  $Fe^{3+}$  state (methemoglobin) (Fig. 3c). Interestingly, pelleted membranes from MEJ fractions were dark brown, consistent with  $Fe^{3+}$  oxidation (Supplementary Fig. 13). We found approximately 32% of Fe existed in the  $Fe^{2+}$  and 68% in the  $Fe^{3+}$  state (Fig. 3d), results that were also sensitive to Hb  $\alpha$  siRNA (Fig 3d). We also observed an increase in NO diffusion in VCCCs treated with CO (Supplementary Fig. 12d).

Previous work has demonstrated that NO-heme  $Fe^{3+}$  interaction results in reductive nitrosylation, a mechanism known to generate S-nitrosothiols, which we have shown to be critical for gap junction regulation at the MEJ<sup>5,24,25</sup>. Using N-acetylcysteine as a bait reactant on the abluminal side (Supplementary Fig. 14a, c), we also found a striking loss of

S-nitrosothiol synthesis after Hb  $\alpha$  knock down in TD arteries (Supplementary Fig. 14b) and in the VCCC (Supplementary Fig. 14d). Together, these results suggest that Hb  $\alpha$  heme oxidation state regulates both NO diffusion and bioactivation.

Next we determined the mechanism regulating Hb  $\alpha$  oxidation state. In erythrocytes, cytochrome B5 reductase 3 (CytB5R3) or diaphorase 1, a known methemoglobin reductase, controls the heme iron oxidation state through reduction of Fe<sup>3+</sup><sup>6</sup>. Using immunofluorescence (*in vivo* Fig 4a, *in vitro* Fig. 4e), TEM (Fig. 4b), and Western blot analysis (*in vivo* Fig. 4c, *in vitro* 4d), we identified that CytB5R3 was expressed in ECs and at the MEJ. In addition, we established CytB5R3 is in a complex with Hb  $\alpha$  using four separate assays: immunofluorescence (Fig. 4f–g), proximity ligation assay (Fig. 4h), and co-immunoprecipitation from cell lysates and purified proteins (Fig. 4i). Indeed, molecular modeling of the crystal structures for Hb  $\alpha$ , eNOS, and CytB5R3 revealed a discreet region of high probability where the proteins could interact (Supplementary Fig. 15). Next, we used CytB5R3 siRNA (knockdown efficiency: ~50%, Supplementary Fig. 16a) and overexpression to show that CytB5R3 regulates metHb  $\alpha$  reduction. Time lapse UV-visible spectrometry demonstrated that loss of CytB5R3 inhibited metHb  $\alpha$  reduction and that overexpression enhanced metHb  $\alpha$  reduction (Supplementary Fig. 16b–c). To determine if CytB5R3 expression or activity regulates arterial tone, we tested both siRNA directed against endothelial CytB5R3 in TD arteries and a pharmacological inhibitor of CytB5R3, propylthiouracil (PTU)<sup>26</sup>. Knockdown efficiency was about 70% (Supplementary Fig. 17a). We observed a decrease in arterial reactivity in TD arteries transfected with CytB5R3 siRNA after PE stimulation with a single dose or cumulative concentrations (Fig. 4j–k) and increased reactivity with ACh dose response (Fig. 4l). Vascular reactivity to PE or Ach in TD arteries pretreated with PTU is shown in (Supplementary Fig. 18a–c). The effect with PTU was not reversible with L-thyroxine supplementation after PE stimulation (Supplementary Fig. 18b, inset). However, we found no change with 5-HT (Supplementary Table 1). EC<sub>50</sub> and E<sub>max</sub> values are in Supplementary Table 2. However, with the addition of L-NAME, the effect of CytB5R3 siRNA was comparable to control conditions (Fig. 4j–l) or PTU treated arteries (Supplementary Fig. 18a–b), results that were consistent with Hb  $\alpha$  knockdown. We found no difference in basal tone for CytB5R3 siRNA or PTU (Supplementary Fig. 11a–b). Next we tested the effect of CytB5R3 on NO diffusion in vessels and VCCC (Fig. 4m, o). Knockdown of CytB5R3 siRNA was ~30% at the MEJ (Supplementary Fig. 17b) and in the EC monolayer but not in SMCs (Supplementary Fig. 17c). Both CytB5R3 siRNA and PTU treatment increased NO diffusion across both isolated vessels and in VCCC (Fig. 4n, p; Supplementary Fig. 18d–g). Note that CytB5R3 knockdown did not alter MEJ eNOS or Hb  $\alpha$  expression (Supplementary Fig. 17d).

We conclude that EC expression of Hb  $\alpha$  plays a critical role in the regulation of NOS-mediated signaling and in the control of arterial vascular reactivity. These results may have far reaching implications that could influence many aspects of vascular biology and disease. For example, endothelial Hb  $\alpha$  expression may participate in blood pressure control, arteriogenesis and anti-inflammatory signaling, as well as impact other redox signaling molecules (e.g. superoxide and hydrogen peroxide). Indeed, our results correlate with diagnostic indices for human alpha thalassemia major (Hb  $\alpha$  <sup>-/-</sup>) fetuses, who show

increased cerebral blood flow during development<sup>27</sup>. Furthermore, these observations may help to explain why inhibition of CytB5R3 attenuates hypertension<sup>28</sup> and may suggest that CytB5R3 is a novel therapeutic target for disease treatment. However, studies devoted toward understanding the mechanisms of CytB5R3 regulation and its interaction with Hb  $\alpha$  will need to be clarified. More broadly, somatic cell types as diverse as alveolar epithelial cells<sup>7</sup>, macrophages<sup>9</sup>, neurons<sup>10</sup> and renal mesangial cells<sup>8</sup> express both Hb and NOS. It is thus possible that Hb could regulate NO signaling pathways relevant to many cell and organ systems. Taken together, these data provide evidence for a novel paradigm in which somatic cell Hb oxidation is required for NO-dependent bioactivity.

## Methods Summary

Human coronary ECs and SMCs were co-cultured and fractionated as previously described<sup>29</sup>. iTRAQ proteomic screening was used to identify and quantify proteins enriched at the MEJ as previously demonstrated<sup>30</sup>. Protein was analyzed using Western blot, immunofluorescence, and immuno TEM, while mRNA was measured using real-time-PCR. Isolated TD arteries were cannulated, pressurized and stimulated with PE or Ach as previously shown<sup>5</sup> or perfused with anaerobic aqueous nitric oxide. Detailed methods can be found in supplementary materials and methods.

## Supplementary Material

Refer to Web version on PubMed Central for supplementary material.

## Acknowledgments

We thank the Advanced Microscopy and Histology core at the University of Virginia and the Yale Proteomic Facility. We acknowledge Vivek Balasubramaniam, Steve Lewis and David Singel for helpful discussions of the data and Brian Duling for critical evaluation of experiments and of the manuscript. We also thank Mitchell Weiss for the Hb  $\alpha$  stabilizing protein antibody and important discussions. This work was supported by an American Heart Association Scientist Development Grant (B.E.I.), National Institute of Health grants HL088554 (B.E.I.), HL107963 (B.E.I.) HL059337 (B.G.), HL101871 (B.G.), HL112904 (A.C.S.), and HL007284 (A.W.L. and A.C.S.). M.B and S.R.J. were supported by American Heart Association postdoctoral fellowships and A.W.L and M.Y.L. were supported by American Heart Association postdoctoral fellowships.

## References

1. Lim KH, Ancrile BB, Kashatus DF, Counter CM. Tumour maintenance is mediated by eNOS. *Nature*. 2008; 452:646–649. [nature06778 \[pii\]](#). [10.1038/nature06778 \[PubMed: 18344980\]](#)
2. Hess DT, Matsumoto A, Kim SO, Marshall HE, Stamler JS. Protein S-nitrosylation: purview and parameters. *Nat Rev Mol Cell Biol*. 2005; 6:150–166. [nrm1569 \[pii\]](#). [10.1038/nrm1569 \[PubMed: 15688001\]](#)
3. Bolotina VM, Najibi S, Palacino JJ, Pagano PJ, Cohen RA. Nitric oxide directly activates calcium-dependent potassium channels in vascular smooth muscle. *Nature*. 1994; 368:850–853. [10.1038/368850a0 \[PubMed: 7512692\]](#)
4. Shesely EG, et al. Elevated blood pressures in mice lacking endothelial nitric oxide synthase. *Proc Natl Acad Sci U S A*. 1996; 93:13176–13181. [\[PubMed: 8917564\]](#)
5. Straub AC, et al. Compartmentalized connexin 43 s-nitrosylation/denitrosylation regulates heterocellular communication in the vessel wall. *Arterioscler Thromb Vasc Biol*. 2011; 31:399–407. [ATVBAHA.110.215939 \[pii\]](#). [10.1161/ATVBAHA.110.215939 \[PubMed: 21071693\]](#)
6. Hultquist DE, Passon PG. Catalysis of methaemoglobin reduction by erythrocyte cytochrome B5 and cytochrome B5 reductase. *Nat New Biol*. 1971; 229:252–254. [\[PubMed: 4324110\]](#)

7. Newton DA, Rao KM, Dluhy RA, Baatz JE. Hemoglobin is expressed by alveolar epithelial cells. *J Biol Chem.* 2006; 281:5668–5676. M509314200 [pii]. 10.1074/jbc.M509314200 [PubMed: 16407281]
8. Nishi H, et al. Hemoglobin is expressed by mesangial cells and reduces oxidant stress. *J Am Soc Nephrol.* 2008; 19:1500–1508. ASN.2007101085 [pii]. 10.1681/ASN.2007101085 [PubMed: 18448584]
9. Liu L, Zeng M, Stamler JS. Hemoglobin induction in mouse macrophages. *Proc Natl Acad Sci U S A.* 1999; 96:6643–6647. [PubMed: 10359765]
10. Schelshorn DW, et al. Expression of hemoglobin in rodent neurons. *J Cereb Blood Flow Metab.* 2009; 29:585–595. jcbfm2008152 [pii]. 10.1038/jcbfm.2008.152 [PubMed: 19116637]
11. Halligan KE, Jourdain FL, Jourdain D. Cytoglobin is expressed in the vasculature and regulates cell respiration and proliferation via nitric oxide dioxygenation. *J Biol Chem.* 2009; 284:8539–8547. M808231200 [pii]. 10.1074/jbc.M808231200 [PubMed: 19147491]
12. Brunori M, et al. Neuroglobin, nitric oxide, and oxygen: functional pathways and conformational changes. *Proc Natl Acad Sci U S A.* 2005; 102:8483–8488. 0408766102 [pii]. 10.1073/pnas.0408766102 [PubMed: 15932948]
13. Fogel U, Merx MW, Godecke A, Decking UK, Schrader J. Myoglobin: A scavenger of bioactive NO. *Proc Natl Acad Sci U S A.* 2001; 98:735–740. 10.1073/pnas.011460298011460298 [pii] [PubMed: 11136228]
14. Dora KA, Doyle MP, Duling BR. Elevation of intracellular calcium in smooth muscle causes endothelial cell generation of NO in arterioles. *Proceedings of the National Academy of Sciences of the United States of America.* 1997; 94:6529–6534. [PubMed: 9177252]
15. Angelo M, Hausladen A, Singel DJ, Stamler JS. Interactions of NO with hemoglobin: from microbes to man. *Methods Enzymol.* 2008; 436:131–168. S0076-6879(08)36008-X [pii]. 10.1016/S0076-6879(08)36008-X [PubMed: 18237631]
16. Gladwin MT, Lancaster JR Jr, Freeman BA, Schechter AN. Nitric oxide's reactions with hemoglobin: a view through the SNO-storm. *Nat Med.* 2003; 9:496–500. 10.1038/nm0503-496nm0503-496 [pii] [PubMed: 12724752]
17. Palmer RM, Ferrige AG, Moncada S. Nitric oxide release accounts for the biological activity of endothelium-derived relaxing factor. *Nature.* 1987; 327:524–526. 10.1038/327524a0 [PubMed: 3495737]
18. Ignarro LJ, Adams JB, Horwitz PM, Wood KS. Activation of soluble guanylate cyclase by NO-hemoproteins involves NO-heme exchange. Comparison of heme-containing and heme-deficient enzyme forms. *J Biol Chem.* 1986; 261:4997–5002. [PubMed: 2870064]
19. Ignarro LJ, Byrns RE, Buga GM, Wood KS. Endothelium-derived relaxing factor from pulmonary artery and vein possesses pharmacologic and chemical properties identical to those of nitric oxide radical. *Circ Res.* 1987; 61:866–879. [PubMed: 2890446]
20. Cassoly R, Gibson Q. Conformation, co-operativity and ligand binding in human hemoglobin. *J Mol Biol.* 1975; 91:301–313. [PubMed: 171411]
21. Doyle MP, Hoekstra JW. Oxidation of nitrogen oxides by bound dioxygen in hemoproteins. *J Inorg Biochem.* 1981; 14:351–358. S0162-0134(00)80291-3 [pii]. [PubMed: 7276933]
22. Eich RF, et al. Mechanism of NO-induced oxidation of myoglobin and hemoglobin. *Biochemistry.* 1996; 35:6976–6983. 10.1021/bi960442gbi960442g [pii] [PubMed: 8679521]
23. Sharma VS, Traylor TG, Gardiner R, Mizukami H. Reaction of nitric oxide with heme proteins and model compounds of hemoglobin. *Biochemistry.* 1987; 26:3837–3843. [PubMed: 3651417]
24. Tejero J, et al. Low NO concentration-dependence of the reductive nitrosylation reaction of hemoglobin. *J Biol Chem.* 2012 M111.298927 [pii]. 10.1074/jbc.M111.298927
25. Angelo M, Singel DJ, Stamler JS. An S-nitrosothiol (SNO) synthase function of hemoglobin that utilizes nitrite as a substrate. *Proc Natl Acad Sci U S A.* 2006; 103:8366–8371. 0600942103 [pii]. 10.1073/pnas.0600942103 [PubMed: 16717191]
26. Lee E, Kariya K. Propylthiouracil, a selective inhibitor of NADH-cytochrome b5 reductase. *FEBS Lett.* 1986; 209:49–51. 0014-5793(86)81082-1 [pii]. [PubMed: 3803575]

27. Lam YH, Tang MH. Middle cerebral artery Doppler study in fetuses with homozygous alpha-thalassaemia-1 at 12-13 weeks of gestation. *Prenat Diagn.* 2002; 22:56–58.10.1002/pd.237[pii] [PubMed: 11810652]
28. Fregly MJ, Hood CI. Physiologic and anatomic effects of prophythiouracil on normal and hypertensive rats. *Circ Res.* 1959; 7:486–496. [PubMed: 13652401]
29. Heberlein KR, et al. Plasminogen activator inhibitor-1 regulates myoendothelial junction formation. *Circ Res.* 2010; 106:1092–1102. CIRCRESAHA.109.215723 [pii]. 10.1161/CIRCRESAHA.109.215723 [PubMed: 20133900]
30. Davalos A, et al. Quantitative proteomics of caveolin-1-regulated proteins: characterization of polymerase i and transcript release factor/CAVIN-1 IN endothelial cells. *Mol Cell Proteomics.* 2010; 9:2109–2124. M110.001289 [pii]. 10.1074/mcp.M110.001289 [PubMed: 20585024]

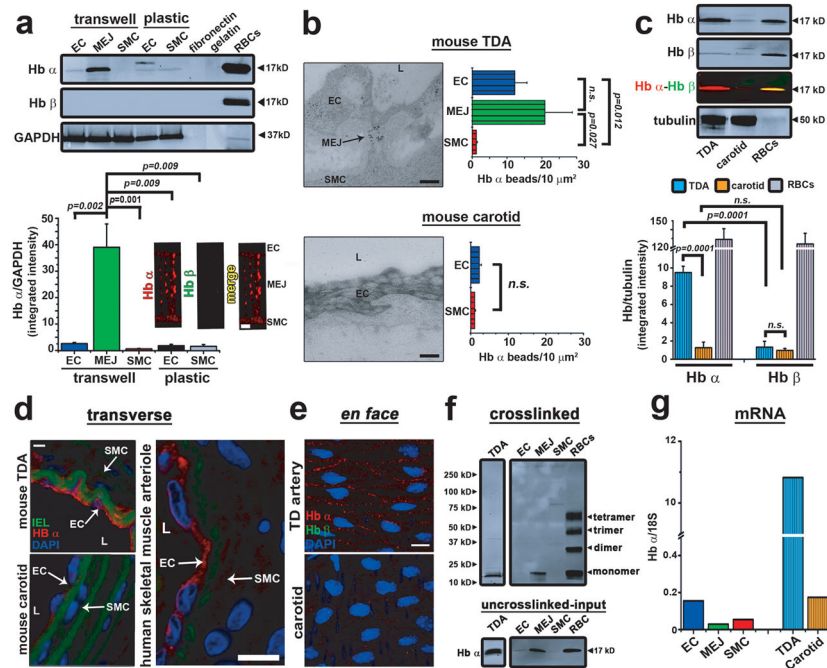


**Figure 1. Monomeric Hb  $\alpha$  is expressed in ECs and enriched at the MEJ**

**a.** Quantitative Western blot analysis for Hb  $\alpha$  and Hb  $\beta$  expression in coronary EC, MEJ or SMC lysates from cells plated on Transwells or plastic (n = 4), or in fibronectin and gelatin used to coat Transwells. Red blood cells served as a positive control and GAPDH was used as loading and normalization control for quantitation (bottom left). Immunofluorescence for Hb  $\alpha$  (red) and Hb  $\beta$  (green) (bottom right). **b.** TEM analysis of Hb  $\alpha$  expression in TD (top) or carotid (bottom) arteries visualized using 10 nm gold beads (black particles). Arrow indicates MEJ. Graphs on the right represent Hb  $\alpha$  localization calculated by measuring the number of beads per  $\mu\text{m}^2$  (n = 7). **c.** Quantitative Western blot analysis for Hb  $\alpha$  and Hb  $\beta$  expression in isolated TD or carotid arteries. Tubulin served as a loading control and red blood cells were used as a positive control (n = 3). **d.** Immunofluorescence of transverse sections from mouse carotid or TD arteries or from a human skeletal muscle arteriole. In all images, red indicates Hb  $\alpha$  expression, green shows internal elastic lamina autofluorescence, and blue specifies nuclei. **e.** *En face* images of Hb  $\alpha$  (red) and Hb  $\beta$  (green) expression in ECs from TD or carotid arteries. Blue staining represents nuclei. **f.** Western blot analysis of TD artery, EC, MEJ, SMC or red blood cell lysates that were chemically crosslinked using BS<sub>3</sub> to determine quaternary structure of Hb  $\alpha$ . **g.** mRNA analysis from EC, MEJ and SMC lysates isolated from VCCC, TD and carotid arteries. 18S was used as a normalization factor. In **a**, **b**, **c**, and **g** open bars represent *in vitro* data and striped bars indicate *ex vivo* data. Scale bar in **a** is 2  $\mu\text{m}$ , **b** is 0.5  $\mu\text{m}$ , **d** indicates 30  $\mu\text{m}$  (TD artery and carotid) or 10  $\mu\text{m}$  (human skeletal muscle artery) and **e** signifies 10  $\mu\text{m}$ . L is lumen (**b**, **d**) and *n.s.* indicates not significant (**b**, **c**) *p* values are shown for each comparison. All error bars represent s.e.m.

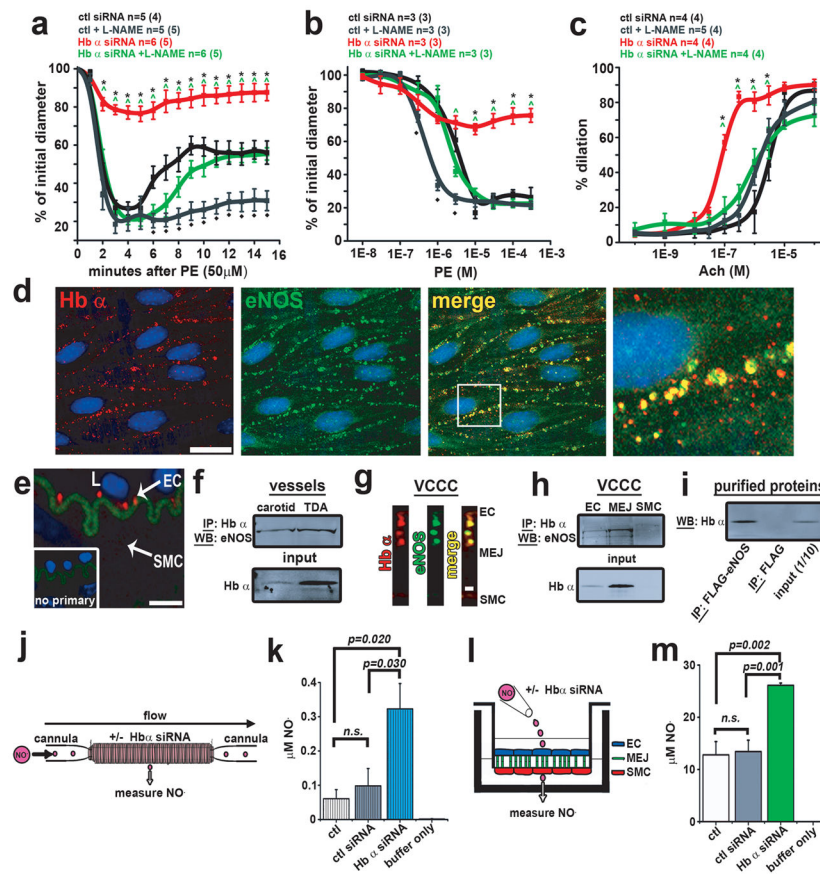


**Figure 2. Hb  $\alpha$  regulates vessel tone, NO diffusion and associates with eNOS**

**a**, Time course to 50  $\mu$ M PE, **b** dose response to PE and **c** dose response to Ach on TD arteries treated with control or Hb  $\alpha$  siRNA in the presence or absence of L-NAME. In **a–c**, n indicates the number of arteries; value in parenthesis shows number of mice. **d**, *En face* view of a dual immunofluorescence of a mouse TD artery showing Hb  $\alpha$  (red) and eNOS (green). The white box in the merge panel indicates the region of interest magnified in the right panel. **e**, Proximity ligation assay for Hb  $\alpha$  and eNOS (red punctates) in transverse mouse TD artery sections. Inset shows the negative control. **f**, Western blot analysis from samples co-immunoprecipitated for Hb  $\alpha$  and blotted for eNOS from isolated TD and carotid arteries. **g**, Dual immunofluorescence for Hb  $\alpha$  and eNOS on transverse section from a VCCC. Red indicates Hb  $\alpha$  and green shows eNOS. **h**, Co-immunoprecipitation of Hb  $\alpha$  Western blotted for eNOS on VCCC lysates. **i**, Co-immunoprecipitation of purified eNOS-FLAG protein blotted for Hb  $\alpha$ . **j**, Schematic diagram of experimental design illustrating a cannulated vessel transfected with Hb  $\alpha$  siRNA showing NO diffusion as a readout. **k**, NO diffusion results from mouse TD arteries transfected with control or Hb  $\alpha$  siRNA (n = 5). **l**, Illustration of experimental setup for VCCC experiments. **m**, NO diffusion results from VCCCs transfected with control or Hb  $\alpha$  siRNA. (n = 4). In **k** striped bars represent *ex vivo* data and in **m** open bars indicate *in vitro* data. In **a–c**, \* shows significance between control siRNA vs. Hb  $\alpha$  siRNA, ^ indicates significance between Hb  $\alpha$  siRNA vs. Hb  $\alpha$  siRNA + L-NAME and ◆ represents significance between control vs. control + L-NAME. In **d–e** scale

bar is 10  $\mu\text{m}$  and in **g** 1  $\mu\text{m}$ . In **k** and **m** *n.s* indicates not significant. In **e**, **L** indicates the lumen *p* values are shown for each comparison. All error bars represent s.e.m.

Author Manuscript

Author Manuscript

Author Manuscript

Author Manuscript

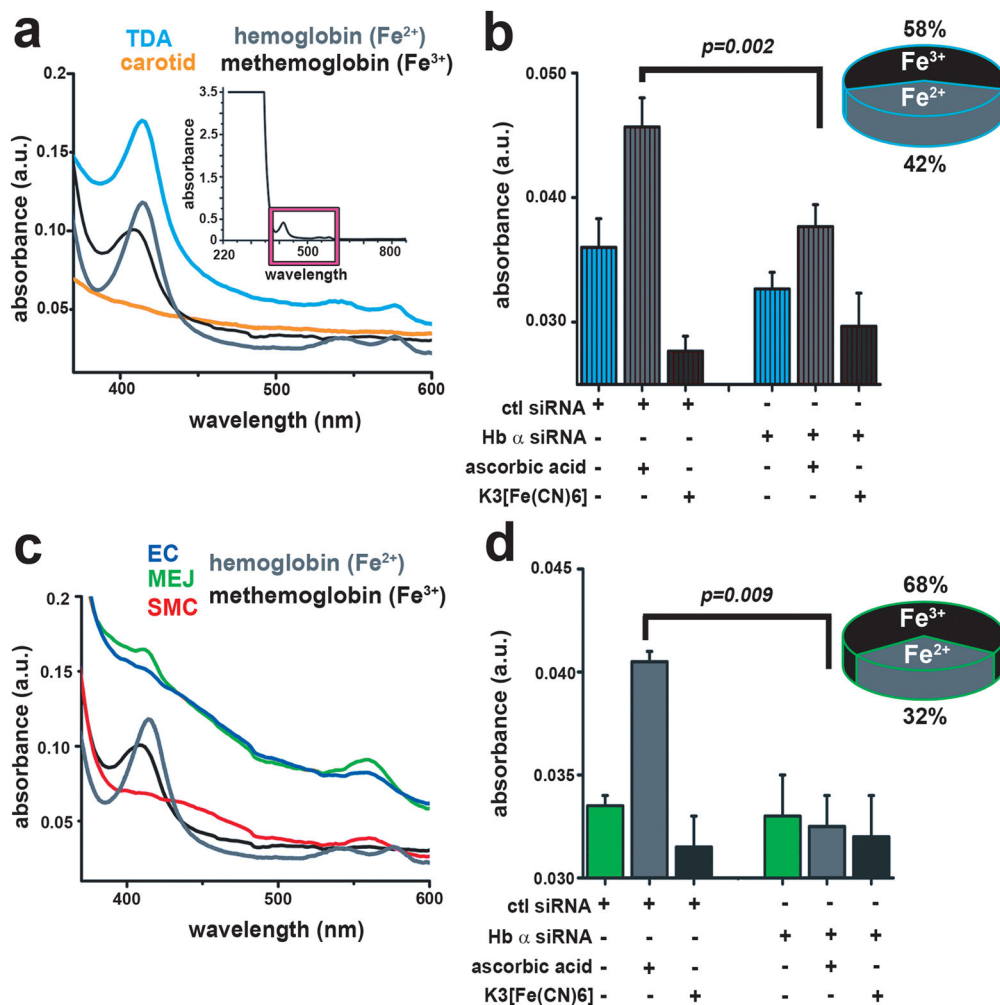


**Figure 3. The oxidation state of Hb  $\alpha$  resides in a mixture of Fe<sup>2+</sup> and Fe<sup>3+</sup>**  
**a**, Ultraviolet-visible spectroscopy analysis of TD arteries and c VCCC fractions. The inset in **a** indicates the region of interest (magenta box) of the Soret (~420 nm) and Q bands (~540–575 nm). **b**, measurement of Hb  $\alpha$  oxidation state calculating the ratio of Fe<sup>2+</sup> to Fe<sup>3+</sup> in TD arteries (n=3) and **d** VCCC fractions (n=3) with and without Hb  $\alpha$  siRNA. In **b** striped bars indicate *ex vivo* data and in **d** open bars represent *in vitro* data. *p* values are indicated for each comparison. All error bars represent s.e.m.

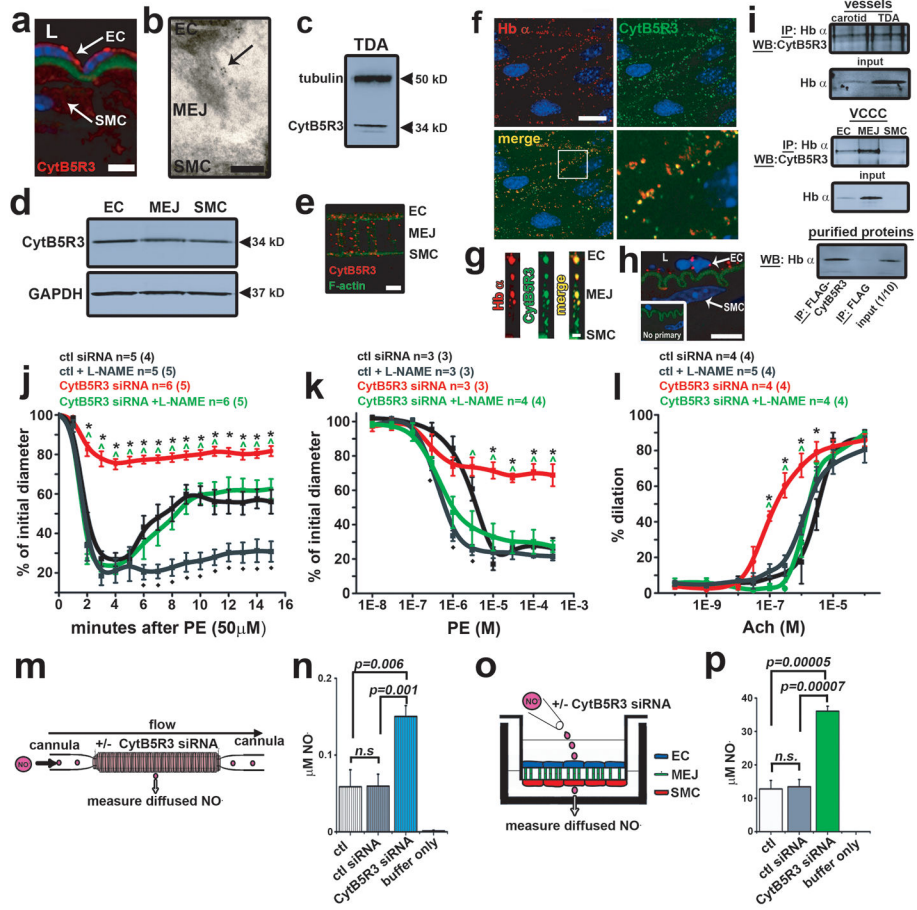


**Figure 4. CytB5R3 expression and activity are critical for vasomotor tone and NO diffusion**  
**a**, Immunofluorescence of CytB5R3 expression (red) and nuclei (blue). Green represents autofluorescence from internal elastic lamina. **b**, TEM analysis of CytB5R3 expression at the MEJ (black particles) *in vivo*. **c**, Western blot analysis of CytB5R3 in TD arteries and **d** in VCCC. **e**, Immunofluorescence of CytB5R3 expression in the VCCC. Red shows CytB5R3 and green indicates F-actin. **f**, *En face* view of a dual immunofluorescence labeling of a mouse TD artery showing Hb  $\alpha$  (red) and CytB5R3 (green) in upper panels. White box in the merge image in the lower left panel shows the region of interest magnified in the lower right panel. **g**, Colocalization of CytB5R3 (red) and Hb  $\alpha$  (green) on a transverse section from the VCCC. **h**, Proximity ligation assay for Hb  $\alpha$  and CytB5R3 (red punctates) on transverse mouse TD artery sections. Inset shows the negative control. Green shows internal elastic lamina autofluorescence. **i**, Western blot analysis from samples co-immunoprecipitated for Hb  $\alpha$  and blotted for CytB5R3 from isolated TD and carotid arteries, VCCC or purified proteins. **j**, Time course to 50  $\mu$ M PE, **k** dose response to PE and **l** dose response to Ach on TD arteries treated with control or Hb  $\alpha$  siRNA in the presence or absence of L-NAME. In **j-l**, n indicates the number of arteries; value in parenthesis shows number of mice. **m**, Schematic of experimental setup for NO diffusion assay in a cannulated artery that was transfected with CytB5R3 siRNA. **n**, Results from NO diffusion experiment in mouse TD arteries with genetic knockdown of CytB5R3 expression (n 3). **o**, Illustration showing the experimental setup for VCCC experiments. **p**, NO diffusion results from

VCCCs transfected with control or CytB5R3 siRNA (n=4). In **n** striped bars indicate *ex vivo* data and in **p** open bars represent *in vitro* data. In **j-l** \* shows significance between control siRNA vs. CytB5R3 siRNA, ^ indicates significance between CytB5R3 siRNA and CytB5R3 siRNA + L-NAME and ♦ represents significance between control vs. control + L-NAME. **a**, Scale bar is 10  $\mu\text{m}$ , **b** is 0.25  $\mu\text{m}$ , **e** is 5  $\mu\text{m}$ , **f, h** are 10  $\mu\text{m}$  and **g** is 1  $\mu\text{m}$ . In **a** and **h**, L indicates lumen *p* values are indicated for each comparison. All error bars represent s.e.m.